SCIENTIFIC PAPER

EXPERIMENTAL VISCOSITY MEASUREMENTS OF BIODIESELS AT HIGH PRESSURE

C. J. Schaschke*

School of Science, Engineering and Technology, Abertay University, Bell Street, Dundee, DD1 1HG, Scotland.

Received 12.2.2016.

Accepted 11.3.2016.

* Corresponding auhor: Tel: 01382 308488; Email: c.schaschke@abertay.ac.uk

Abstract

The viscosity of biodiesels of soybean and rapeseed biodiesels blended with mineral diesel fuel were measured at pressures of up to 200 MPa. Using a falling sinker-type viscometer reproducible viscosity data were obtained based on the time taken for a sinker to descend a fixed distance down an enclosed tube under the influence of gravity. Measurements were taken using pressures which correspond to those of interest in automotive common rail diesel engines, and at temperatures of between 25^{o}C and 80^{o}C. In all cases, the viscosity of the biodiesel blends were found to increase exponentially for which the blends were noted as being more viscous than pure mineral fuels. A pressure-freezing effect was not observed for the blends.

Keywords: *Falling sinker viscometer, high-pressure, biodiesel, viscosity, rapeseed, soybean*

Highlights:

- High pressure viscosity measurements of biodiesel blends using a falling sinker-type viscometer.
- Pressures applied up to 200 MPa covers the range used in modern common rail diesel engines.
- The combined effects of both temperature and pressure on the blends is examined.
- Two parameter Barus model used to describe each viscosity profile for each isotherm with good fit.
- The data presented o a growing body of data relevant to automotive engine manufactures.

Introduction

Biodiesels derived from renewable sources are increasingly being blended with petrochemical or "mineral" diesels for use as fuels for compression-ignition type automotive engines. Biodiesels as fuels are attractive offering a number of benefits in terms of meeting exhaust emission requirements and, significantly, their use in existing engines without the need for modification. A concern, however, is their higher viscosity than mineral biodiesels [1].

The synthesis of biodiesel is relatively straightforward involving the transesterification of any natural oil or fat with an alcohol into fatty acid methyl esters or FAME. The principal benefit of this biofuel is its environmental impact in comparison with mineral diesel [2]. Comprising long-chain fatty acid methyl esters, the composition of FAME is dependent on the raw materials used. As a fuel in its own right, FAME tends not to be used as a pure fuel but instead is as a blend with mineral diesel. B100 comprises entirely biodiesel whereas B10 and B15, for example, comprise 10% and 15% biodiesel with the remainder (90% and 85%, respectively) being mineral diesel.

The fact that biodiesel can be produced not only from renewable agricultural sources such as rapeseed, soybean and palm seed oils, but also from waste oils, makes biodiesel an attractive and versatile contender for the renewable replacement of mineral diesel. Being sulphur-free, the combustion of biodiesel has the benefit of not giving rise to harmful sulphur oxides and sulphates. Further, as a solvent, biodiesel is also effective at removing diesel deposits that may accumulate in the fuel tank and also provides essential lubricating properties that reduce engine wear [3].

The calorific value of biodiesel is dependent on the source material. Values vary depending on the feed source but typical values are in the order of 40 MJ kg^{-1} compared to mineral diesel, which has a calorific value of 47 MJ kg^{-1} depending on the composition. The energy release through combustion of 1 kg of the biodiesel and mineral diesel is equivalent to 11.1 kWh and 13.0 kWh, respectively. A B10 and B15 blend, for example, would therefore typically have a fuel equivalent value of 12.8 kWh and 12.7 kWh, respectively.

Used as a fuel used in common rail automotive diesel engines, which typically operate at pressures of between 140 and 160 MPa, injector nozzles ensure rapid atomisation and combustion of the fuel thus providing efficient combustion and low particulate emissions [4]. The viscosity of the fuel is an important parameter for atomisation through the injector. This is achieved effectively at high pressure and has resulted in the common rail automotive engine revolutionising diesel engine technology.

Under high pressure injection conditions, the density, viscosity and lubricity of the fuel may vary significantly. Compared to mineral diesel data, there is a low but steadily growing body of available data on the properties of biodiesels with pressure [5-7]. The effect of methyl esthers is known to influence the lubricity of the biodiesel fuels [8]. The presence of free fatty acids (FFAs) and diacylglycerols can also affect lubricity although to not the same extent as monoacylglycerols and triacylglycerols, which have virtually no effect [3]. The work presented here adds to the viscosity data of biodiesel blends as Rapeseed Methyl Ester (RME) and Soybean Methyl Ester (SME) using a high pressure falling sinker-type viscometer at pressures of up to 200 MPa. The viscometer comprises a vertical tube down in which a close-fitting self-centring sinker descends under the influence of gravity with the viscosity data being obtained from sinker fall times captured electronically.

Experimental

The synthesis of biodiesels can follow several established process routes [10, 11]. The biodiesels used in this study were based on rapeseed and soybean and produced by transesterification with methanol to form Rapeseed Methyl Ester (RME) and Soybean Methyl Ester (SME). The mineral diesel used was supplied directly from a British refinery and combined with the biodiesels to form B10 and B15 blends. That is, blends of 10% and 15% biodiesel to the remainder as mineral diesel.

The transesterification process involves the reaction of triacylglycerols or esterification of small amounts of free fatty acids (FFAs) with alcohol in the presence of an acid or alkali catalyst to form glycerol and fatty acid methyl esters (FAME), otherwise known

as biodiesel. After separation from the glycerol, the biodiesel was then purified ready for use. The transesterification reaction requires a catalyst since spontaneous reaction between alcohol and oil is very slow. The catalyst therefore promotes transesterification and formed diacylglycerol and monoacylglycerol during the initial period of transesterification also increases the solubility of methanol and oil thus permitting the reaction to proceed at a reasonable rate. The reaction may, however, not be complete should the operating temperature fall below that required for the reaction, or should the processing time be insufficient. In such case, reaction mixture at the end of transesterification may also contain smaller or significant concentrations of diacylglycerols and monoacylglycerols. Diacylglycerols are known to be responsible for coking in engines while monoacylglycerols are responsible for causing corrosion and require to be kept at a combined concentration of less than 0.1%.

To date, the viscosity data for biodiesels and their blends with mineral fuels has been obtained using various types of instruments. While the majority of rheometers operate at atmospheric pressure over a wide range of shear rates and shear stresses, the measurement of viscosity at elevated pressures, however, is not quite so straightforward due to the need for high pressure containment of the instrument. Several designs of high-pressure viscometer exist ranging from a few tens to thousands of bar pressure in operation. In each case, the design is challenged with the need for adequate sealing and the ability to detect movement. Rolling ball, vibrating wire and torsionally vibrating crystal methods are noted for their successful measurement of the viscosity of complex organic fluids such as alkanes at high pressure operate which use sapphire windows or electronic sensors as ways of detecting movement within [12].

In this work, a falling sinker viscometer was used. The instrument consists of a vertical tube containing the fluid under examination down in which a close fitting sinker descends under the influence of gravity. The sinker is allowed to descend through the fluid being tested reaching its terminal velocity as a balance of forces between the gravitational pull on the sinker, its buoyancy and shear stress within the narrow gap between the sinker and viscometer tube wall [13]. The entire viscometer is contained within a high pressure chamber filled with a pressure-transmitting hydraulic oil. The

necessary pressure was generated by way of a pressure intensification unit using compressed air at a pressure of around 1 MPa and amplified to a maximum target operating pressure of 200 MPa. The hydraulic pressure was transmitted to the biodiesel fluids under examination by way of a flexible PTFE expansion sheath, which also allows for compression of the biodiesel.

The viscometer tube was housed within a pressure vessel rated to a maximum pressure of 1000 MPa and maintained at a constant temperature by immersion in a bath of mono-ethylene glycol. The sinker was positioned ready for descent down the viscometer tube by inversion of the pressure vessel. Each measurement of viscosity began by inversion of the vessel. There is a sufficient fall distance for the sinker to achieve terminal velocity for which the signal captured was in the form of two electronically captured peaks each corresponding to the position of the sinker with its embedded ferrite core inducing a current through coils of copper wire surrounding the outside of the viscometer tube. Consisting of around 200 turns of lacquered copper wire, both coils formed the active arm of a balanced bridge circuit for which the out-of-balance signal from the bridge is amplified and captured on a PC data-logger. On completion of the fall test, the entire pressure vessel was re-inverted to return the sinker to its original starting position in preparation for the next measurement. Typical fall times ranged from tens of seconds to tens of minutes.

A pressure intensifier was used to raise the hydraulic pressure in the vessel and thus sample being tested. The actual pressure achieved within the vessel, and therefore exerted on the fluid being tested, was measured by a calibrated Kistler piezo-resistive pressure gauge type 4618A0. The pressure, p, measured in MPa was related to the voltage output, V_o, in volts, by:

$$p = 47V_o\left(1+\left(\frac{0.0865}{V_o}\right)^{0.675}\right) \qquad (1)$$

The sinker descends the tube concentrically. Self-centring descent has been shown to occur experimentally and is attributed to the close tolerance of the tube and sinker [13].

Spurious shorter sinker fall times are produced where self-centring occasionally does not occur. These data are quickly identified, discounted and the measurement repeated. This may occur, for example, where the sinker descends eccentrically down the inside of the tube wall.

From the size, geometry and buoyancy of the sinker in the tube containing a test fluid, the theoretical dynamic viscosity can be determined from the free descent of the sinker with assumed laminar flow under the influence of gravity as the time taken for the sinker to pass the detection coils [13]. In practice, however, there are permanent energy losses in the form of vortices which shed from the sinker even though the flow through the annual gap between the sinker and tube confirmed to be laminar with a low (modified) Reynolds number of typically single digits. The existence and shedding of vortices has been previously been confirmed both experimentally and by using computational fluid dynamics [14].

The basic equation for dynamic viscosity that allows for compression by pressure as well as thermal expansion is given by [15]:

$$\eta = \frac{t(1-\rho_L/\rho_S)}{A\left(1+\alpha(T-T_o)\right)\left(1-2\beta\left(p-p_o\right)\right)} \tag{2}$$

To minimise compressibility and thermal expansion effects, the sinker and the tube were fabricated from a single bar of En58J non-magnetic steel. More simply, the dynamic viscosity is presented by:

$$\eta = \frac{t}{A}\left(1-\frac{\rho_L}{\rho_S}\right) \tag{3}$$

where the coefficient *A* is based on the physical dimensions of the sinker and tube given by:

$$A = \frac{2\pi L_s L_t}{mg\left(\ln\left(\frac{R_2}{R_1}\right) - \frac{R_2^2 - R_1^2}{R_2^2 + R_1^2}\right)} \quad (4)$$

The variation of the viscometer coefficient as a result of the discrepancy between the theoretical and actual viscosity measurements was therefore examined using a range of fluids with known viscosity and density data at high pressure shown in Figure 1.

Figure 1

Fluids with a high viscosity provide longer sinker fall times and exhibit correspondingly lower modified Reynolds numbers. The form of Reynolds number for a displaced fluid through the annulus has been previously shown [15] to be of the form:

$$\mathrm{Re}_m = \frac{2\rho_L v_S R_1^2}{\eta\ (R_1 + R_2)} \quad (5)$$

The coefficient has a tendency towards a constant value at low Reynolds number tending towards the theoretical value determined from the dimensions of the tube and sinker, fitted by:

$$A = A_o\left[1 + \left(\frac{B}{t(1 - \rho_L / \rho_S}\right)^N\right] \quad (6)$$

where *Ao* is the limiting constant for an infinite sinker fall time and determined from Equation 4 to be 3.8 Pa^{-1}. N and B are constants.

An important parameter in the determination of viscosity is fluid density. There is an abundance of published density data for pure substances with temperature and pressure. For more complex fluids including mixtures and blends, however, the density variation with temperature and pressure can be predicted in many cases using Equations of States or computed using various published correlations [16]. Experimental measurements

may also be used such as the use of micro-pVT devices or collapsible bellows involving calibration of fluids with known density profiles. In this study, the density of biodiesel with pressure was computed using a modified Tait equation [17].

The prepared viscosity of the biodiesel blends B10 RME, B10 SME, B15 RME and B15 SME were measured using a high-pressure falling sinker viscometer up to pressures of up to 200 MPa (Figures 2-5). The pressure vessel, hydraulic fluid, viscometer tube and biodiesel were maintained at controlled temperatures of 25°C, 40°C 60°C and 80°C. The viscosities at elevated pressure were obtained from direct measurement of the sinker fall times.

Discussion

In general, the viscosity of fluids tends to increase with molecular complexity. This is particularly the case with organic liquids such as polymers and oils in which the more complex the molecular structure, the larger is the effect of pressure. Applied to biodiesels, a number of empirical models have been presented to predict the temperature dependence of viscosity [18-21]. In terms of the effect of pressure on viscosity, the Barus law is the most well-known and established form of relationship (Equation 9) that was first presented in 1893 [22] and has been successfully applied to the experimental data of many fluids.

$$\eta = \eta_O \exp^{\beta p} \tag{7}$$

As with temperature dependence, the longer and more complex the structure, the higher the viscosity with elevated pressure. Diesel fuels and FAME are highly complex in composition and comprise of long chain molecules. The exponential increase in viscosity is therefore to be expected due to the increasing compression of the molecules with pressure inhibiting or restricting molecular movement [23]. In this study, the experimental results indicated that the viscosity of all the fluids and their blends increased with pressure.

The viscosity measurements for each of the biodiesel blends were found to be influenced by both temperature and pressure (Figure 2-5). A number of expanded correlations have been presented that combine elevated temperatures with pressure such as the multi-parameter correlation for di-2-ethylhexel sebecate, which is considered to be a representative substance of biodiesel [17]:

$$\eta = \exp\left(-2.3671 + 0.007672p + \frac{4.327T_{o(p)}}{T - T_{o(p)}} \right) \quad (8)$$

where

$$T_{o(p)} = 162.9 + 0.1088p - 0.0003762p^2 \quad (9)$$

Figures 2, 3 4 5

In this work, the simple two parameter correlations with pressure for each indicated temperature presented in Table 1 were considered to be more useful, for which the correlation coefficient, R^2, with data in all cases was better than a value of 0.999, justifying the more elementary form.

The effects of adiabatic heating during compression on the accuracy of the measurements were ignored since the vessel and viscometer were maintained under isothermal conditions. A sufficient period of time was permitted to attain thermal equilibrium between changes of pressures. Besides, the effects of adiabatic heating may reasonably be assumed to be minimal since the mass and heat capacity of the pressure vessel and viscometer, and the time of pressurisation far outweigh the thermophysical properties of the test fluids considered.

The viscosities of each of the biodiesel blends were found to increase up to 200 MPa across the temperature range. This was indicated by an increase in time for the sinker to pass the two detection coils. A pressure-induced liquid-solid phase change is known to occur for longer chain molecules [24]. This phenomenon has been previously found to

occur with diesel fuels and vegetable oils in which pressure-freezing phase transition of long chained molecules was visually confirmed on depressurisation of the pressure vessel at which the solid material would revert to its liquid state [15, 25]. The implication for high pressure automotive engines may be fuel blockage particularly on cold starts. The dynamic nature of solidification, however, is unlikely to be a cause for concern in operating engines due to their high temperature environment.

The high pressure viscometer is noted for its simplicity and ability to reproduce fall-time data. Relying on the action of gravity and a self-centring action for the sinker to pass two detection coils, the sinker is assumed to reach terminal velocity prior to reaching the coils. This is a reasonable assumption due to a sufficient length of fall prior to reaching the first detection coil. With modified Reynolds numbers typically being in the order of single digits, sinker velocities do not exceed 1.0 mm s^{-1} for the least viscous regimes corresponding to ambient pressure and highest temperature used. The time to reach the detection coils from the sinker start point is therefore no longer than 30 seconds.

Designed to be self-centring during fall, stable positions other than the concentric descent of the sinker exist within the tube [26-29]. These include an eccentric descent along the tube wall. Such eccentric descents are identified by anomalous fall times and are readily discounted.

A calibration curve (Figure 1) was used to allow for the discrepancy between the theoretical sinker fall time and the actual fall time. While it is not possible to visually observe the sinker within the pressure vessel, the existence of vortex shedding is known to occur from both physical testing using a glass tube and sinker with coloured liquid operated at atmospheric pressure as well as using CFD analysis. The use of various calibration fluids of known flow properties illustrate that the three parameter calibration curve (Equation 6) is a reasonable fit. The coefficient can be extrapolated to a zero modified Reynolds number corresponding to the value determined from the physical dimensions of the sinker and tube (Equation 4).

The determination of viscosity data also relies on the variation of density of the test fluid as well as the materials of the sinker and tube. The sinker and tube were fabricated from the same material to reduce variation between the two although allowance was made for compression and thermal expansion in the calculation (Equation 2). Between each test thermal equilibrium was permitted to be attained over a period of an hour to ensure isothermal conditions were met. Allowances to the calculations with coefficients of thermal expansion and pressure compression were made. While the effect of compressibility on the density on the test fluids can be obtained from experimental methods such as the use of micro-pVT and oscillating tube densitometers [30], a modified Tait equation was used in this work. Where published data does not exist, experimental methods are unavailable, or correlations are not valid, Equation 3 can alternatively be used by using several data points and solving simultaneously although there are inherit errors in the both the determined viscosity and density by this method.

Conclusions

The dynamic viscosities of several biodiesel fuels as blends with mineral diesel were been found to increase exponentially with both increasing pressure whilst decreasing temperature. The viscosities were found to be greater than that of mineral diesels alone. The accuracy of the data requires careful selection of a self-centring sinker and need for its calibration prior to testing. The demand for accurate liquid biofuel data with pressure and temperature is essential if determined viscosity data is to be of value particularly in the performance of automotive common rail diesel engines.

Acknowledgements

The technical support of Mr J. Murphy (University of Strathclyde) and Mr Robert Campbell (Abertay University) is also gratefully acknowledged.

Nomenclature

A calibration constant for viscometer, mPa^{-1}

A_o constant for viscometer, 3.8 mPa^{-1}

B sinker constant = 2

g gravitational acceleration, m s^{-2}

L_S sinker length 14.2 mm

L_T sinker fall distance 31.0 mm

m sinker mass, kg

N sinker constant = 2

p pressure, MPa

p_o reference pressure (0.1 MPa)

R^2 correlation coefficient, (-)

Re_m modified Reynolds number, (-)

R_1 radius of sinker, 3.710 mm

R_2 inner tube radius 3.898 mm

T temperature, K

T_o ambient temperature, 298 K

t sinker fall time, s

v_S terminal velocity of sinker, m s^{-1}

V_o voltage, V

Greek symbols

α thermal expansion coefficient 1.4×10^{-5} K^{-1}

β sinker compressibility 2.0×10^{-6} MPa^{-1}

β reciprocal pressure coefficient, MPa

η dynamic viscosity, mPa s

η_o dynamic viscosity at ambient pressure, mPa s

ρ_L sample liquid density, kg m^{-3}

ρ_S sinker density: 5030 kg m^{-3} (at T_o and p_o)

References

1. M. Tat, J. Van Gerpen, J. Am. Oil Chem. Soc. 76 (1999) 1511-1513.
2. R. Srivastas, R. Prasad, Renewable Sustainable Energy Rev. 4 (2002) 111-113.
3. K. Wadumesthrige, A. Mahbuba, S. Salley, K. Ng, Energy Fuels 23 (2009) 2229–2234.
4. S. Lee, D. Tanaka, J. Kusaka, Y. Daisho, JSAE Rev. 23 (2002) 407-414.
5. R. Ferrari, V. Oliveira, A. Scabio, A. Sci. Agric. 62 (2005) 291-295.
6. H. Imahara, E. Minami, S. Saka, Fuel 85 (2006) 1666-1670.
7. Q. Shu, B. Yang, J. Yang, S Qing, Fuel 86 (2007) 1849-1854.
8. G. Knothe, R. Kevin, Energy Fuels 19 (2005) 1192–1200.
9. J. Hu, Z. Du, C. Li, E. Min, Fuel 84 (12-13) (2005) 1601–1606.
10. J. Van Gerpen, Fuel Process. Technol. 86 (2005) 1097-1107.
11. J. Marchetti, V. Miguel, A. Errazu, Renewable Sustainable Energy Rev. 11 (2007) 1300-1311.
12. D. Caudwell, J. Trusler, V. Vesovic, W. Wakeman, Int. J. Thermophys. 25 (2004) 1339-1352.
13. G. Fulin, F. Thomas, J. Irving, Int. J. Heat Mass Transfer 37 (1994) 41–50.
14. C. Schaschke, S. Abid, I. Fletcher, M. Heslop, J. Food Eng. 87 (2008) 51-58.
15. S.C. Vant, PhD thesis, University of Strathclyde, Department of Chemical & Process Engineering, Glasgow, UK (2003).
16. M. Huber, E. Lemmon, A. Kazakov, L. Ott, T. Bruno, Energy Fuels 23 (2009) 3790–3797.
17. X. Paredes, O. Fandiño, A. Pensado, M. Comus, J. Fernández, J. Chem. Thermodyn. 44 (2012) 38-43.
18. K. Krisnangkura, T. Yimsuwan, R. Pairintra, Fuel 85 (2006) 107–113.
19. G. Knothe, K.R. Steidley, Fuel 86 (2007) 2560–2567.
20. W. Yuan, A.C. Hansen, Q. Zhang, Fuel 88 (2009) 1120–1126.
21. E. Blangino, S.D. Romano, Adv. Mater. Res. 236-238 (2011) 3032-3036.
22. C. Barus, Am. J. Sci. 45 (1983) 87–96.
23. K. Kioupis, E. Maginn, J. Phys. Chem. B, 104 (2000) 7774-7783.
24. M. Costa, L. Boros, J. Coutinho, M. Krähenbühl, A. Meirelles, Energy Fuels 25 (2011) 3244–3250.

25. C. Schaschke, S. Allio, E. Holmberg, Trans. Inst. Chem. Eng. Part C 84 (2006) 173–178.
26. M. Chen, J. Lescarboura, G. Swift, AIChE J. 14 (1968) 123-127.
27. J. Irving, J. Phys. D: Appl. Phys. 5 (1972) 214–224.
28. N. Park, T. Irvine, Rev. Sci. Instrum. 66 (1995) 3982–3984.
29. N. Cristescu, B. Conrad, R. Tran-Son-Tay, R. Int. J. Eng. Sci. 40 (2002) 605–620.
30. R. Chang, M. Moldover, Rev. Sci. Instrum. 67 (1996) 251-256.

Figure captions:

Figure 1. Variation of viscometer coefficient with various calibration fluids. ▲Sebecate, □ iso-octane, ○ 100% mineral diesel; ●B100 SME, ■ B100 RME

Figure 2. Variation of viscosity with temperature and pressure for B10 RME. Key: ♦ 25 ^{o}C ■ 40 ^{o}C ▲ 60 ^{o}C ●80 ^{o}C

Figure 3. Variation of viscosity with temperature and pressure for B10 SME. Key: ♦ 25^{o}C■ 40 ^{o}C ▲ 60 ^{o}C ●80 ^{o}C

Figure 4. Variation of viscosity with temperature and pressure for B15 RME. Key: ♦ 25 ^{o}C ■ 40 ^{o}C ▲ 60 ^{o}C ●80 ^{o}C

Figure 5. Variation of viscosity with temperature and pressure for B15 SME. Key: ♦ 25 ^{o}C ■ 40 ^{o}C ▲ 60 ^{o}C ●80 ^{o}C

Table 1 Viscosity correlations with pressure for B10 and B15 blends. $R^2 > 0.999$ in all cases.

Temp ^oC	*Diesel*	*Biodiesel*	*Biodiesel*	*Blend*			
	B0	B100 (RME)	B100 (SME)	B10 RME	B10 SME	B15 RME	B15 SME
25	$\eta=3.198e^{0.0121p}$	$\eta=4.540e^{0.0140p}$	$\eta=4.450e^{0.0140p}$	$\eta=4.247e^{0.0143p}$	$\eta=4.179e^{0.0145p}$	$\eta=4.275e^{0.0131p}$	$\eta=4.302e^{0.0130p}$
40	$1.993e^{0.0096p}$	No data	No data	$\eta=3.482e^{0.0128p}$	$\eta=3.013e^{0.0125p}$	$\eta=2.943e^{0.0116p}$	$\eta=2.999e^{0.0118p}$
60	$1.436e^{0.0081p}$	No data	No data	$\eta=2.057e^{0.0117p}$	$\eta=2.054e^{0.0114p}$	$\eta=2.022e^{0.0104p}$	$\eta=2.090e^{0.0107p}$
80	$0.0973e^{0.0077p}$	No data	No data	$\eta=1.582e^{0.0106p}$	$\eta=1.544e^{0.0108p}$	No data	$\eta=1.595e^{.01080p}$

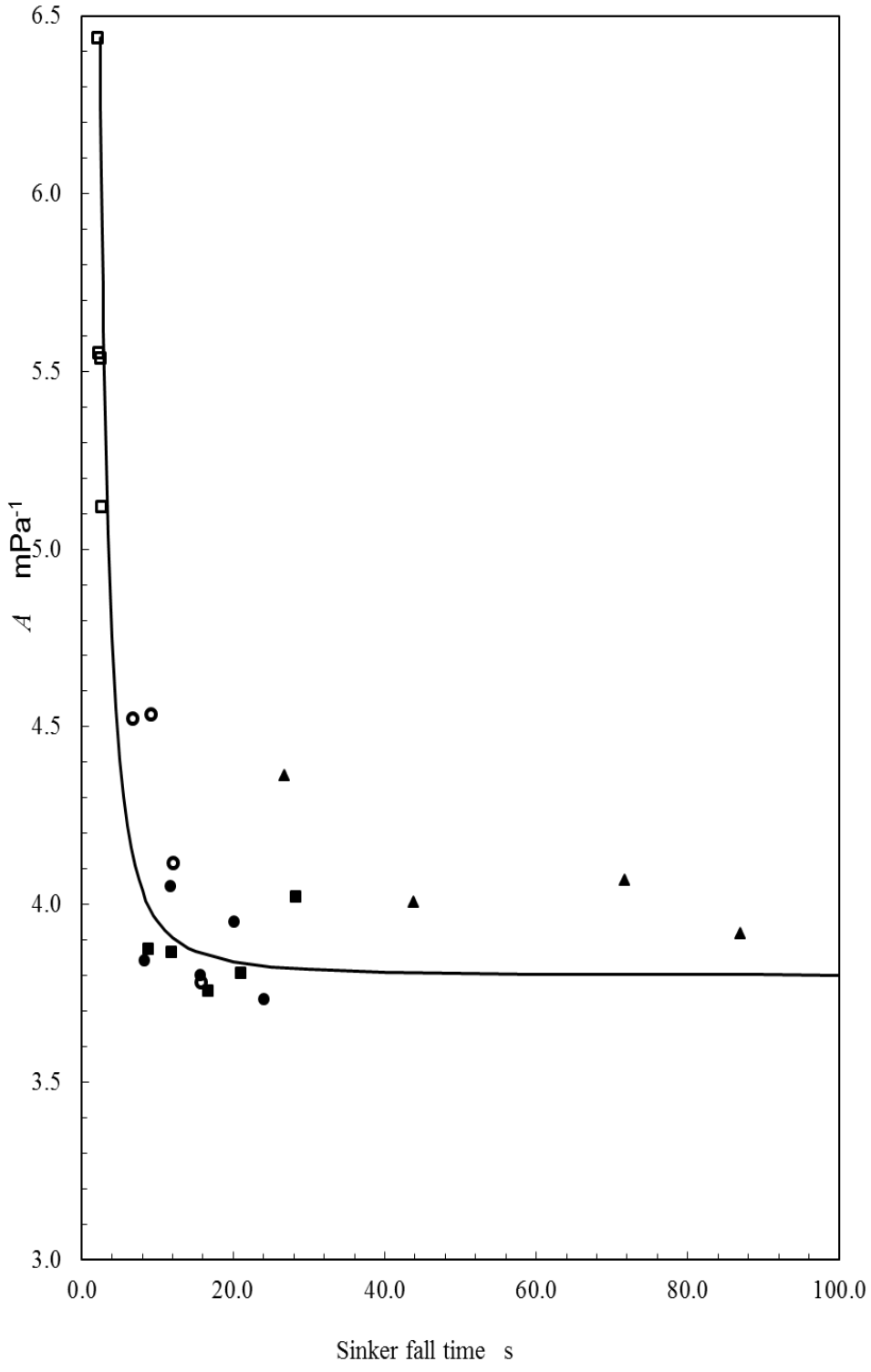

Figure 1. Variation of viscometer coefficient with various calibration fluids. ▲Sebecate, □ iso-octane, ○ 100% mineral diesel; ●B100 SME, ■ B100 RME

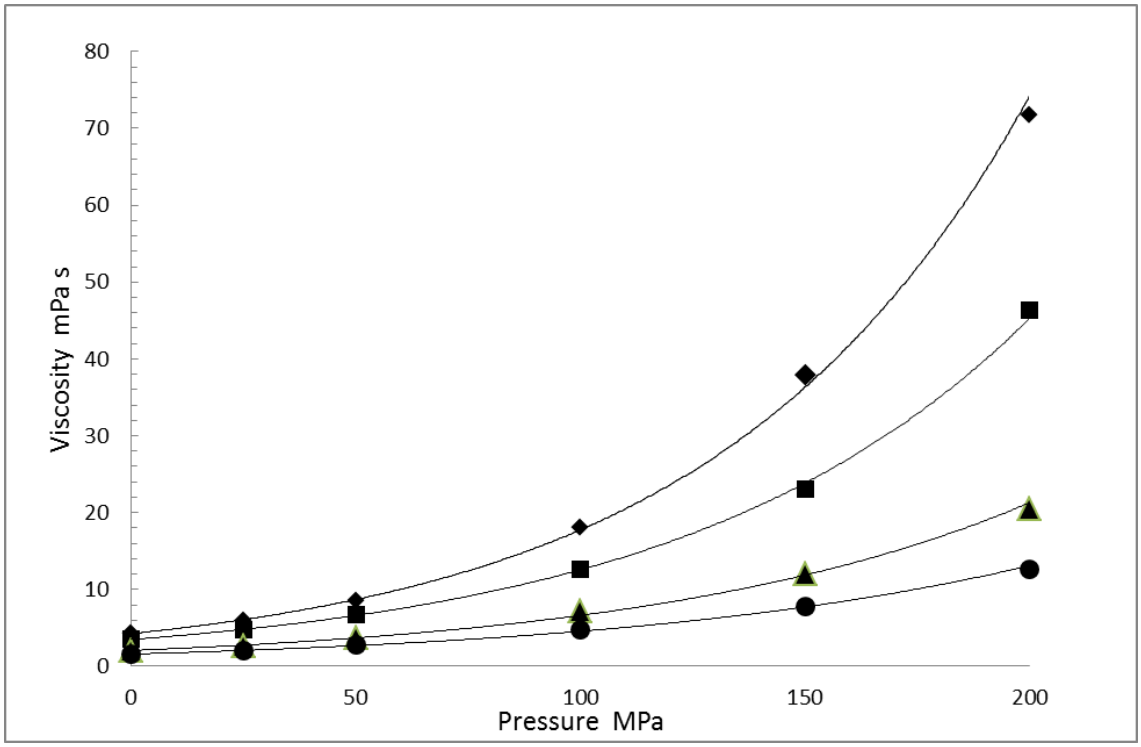

Figure 2. Variation of viscosity with temperature and pressure for B10 RME. Key: ♦ 25 ^{o}C ■ 40 ^{o}C ▲ 60 ^{o}C ●80 ^{o}C

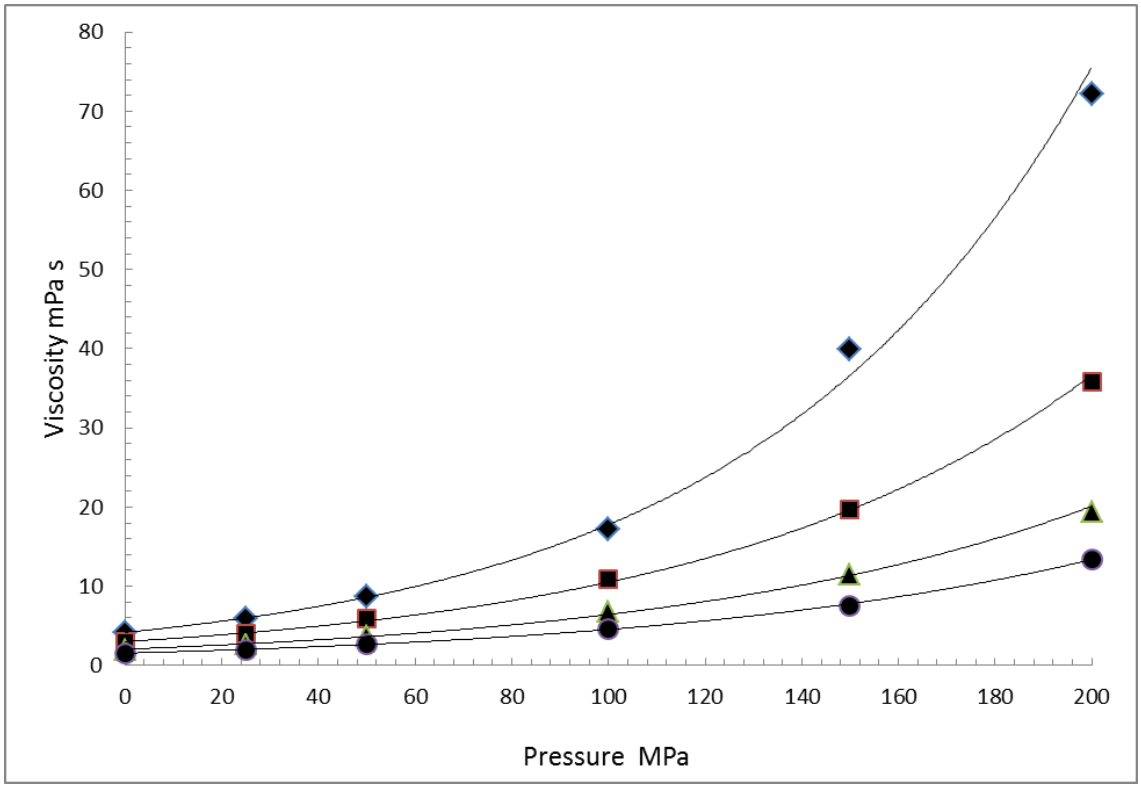

Figure 3. Variation of viscosity with temperature and pressure for B10 SME. Key: ♦ 25°C■ 40 °C ▲ 60 °C ●80 °C

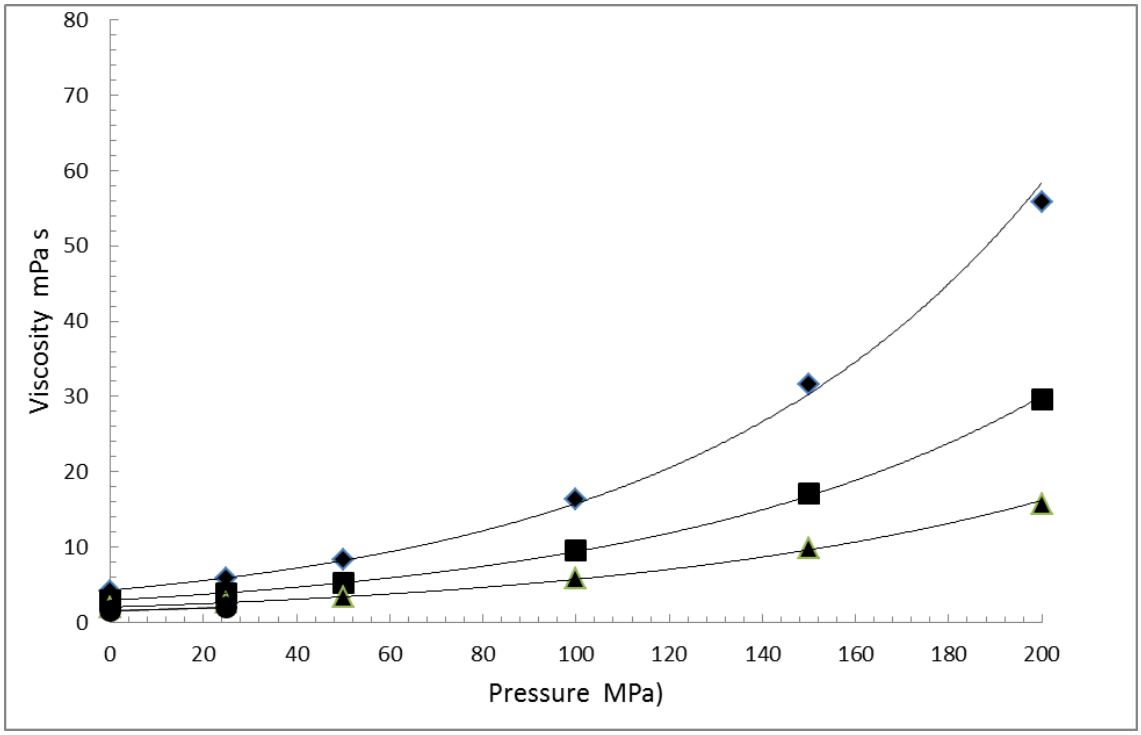

Figure 4. Variation of viscosity with temperature and pressure for B15 RME. Key: ♦ 25 ^{o}C ■ 40 ^{o}C ▲ 60 ^{o}C ●80 ^{o}C

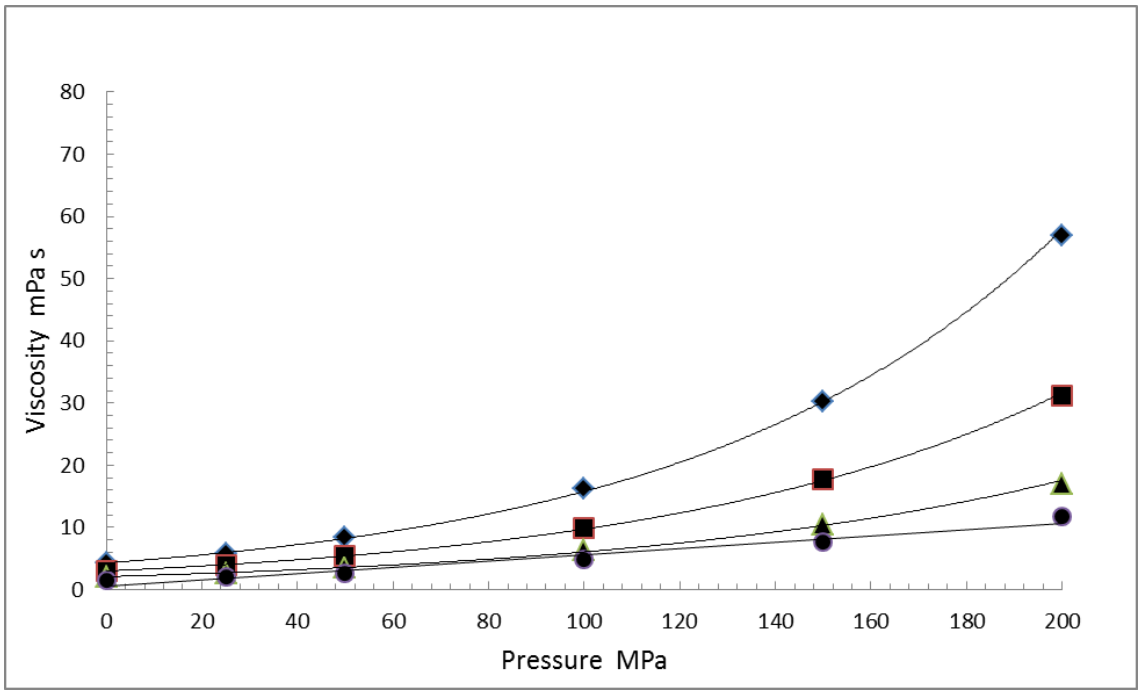

Figure 5. Variation of viscosity with temperature and pressure for B15 SME. Key: ♦ 25 ^{o}C ■ 40 ^{o}C ▲ 60 ^{o}C ●80 ^{o}C